Mechanics & Industry **22**, 27 (2021)
© H. Li et al., published by EDP Sciences 2021
https://doi.org/10.1051/meca/2021026

Mechanics & Industry

Available online at:
www.mechanics-industry.org

REGULAR ARTICLE OPEN ACCESS

A research on aerodynamic characteristics of non-pneumatic tire

Hong Li*, Yilun Xu, Chenlong Si, and Yong Yang

School of Mechanical Engineering Yangzhou University, Yangzhou Jiangsu 225127, China

Received: 9 October 2020 / Accepted: 20 March 2021

Abstract. Application of non-pneumatic tire (NPT) has been increased during the last decade. The aerodynamic characteristics of the wheel with NPT has been studied due to significance on improvement of handling and reduction of fuel consumption. In this paper, first, an original NPT model was simulated by CATIA software, and the influence of NPT structural parameters on aerodynamic characteristics was studied by Fluent software. The simulation calculation results showed that: the reduction of tire width and spoke length, and the increase of spoke thickness can effectively decrease aerodynamic coefficient. Then, the MIRA model was used to study the influence of NPT on aerodynamic characteristics of the whole vehicle under driving conditions. Studies showed that: NPT increased the resistance of the whole vehicle, and 63.1% of the resistance at the wheels was provided by the front wheels. Finally, the wind tunnel test was conducted to study aerodynamic characteristics of the optimized NPT model under static conditions and verify the simulation calculation.

Keywords: NPT / aerodynamic characteristics / structural parameters / wind tunnel test

1 Introduction

Pneumatic tire has occupied the tire market for over 100 years because of the advantages of good shock absorption, low contact pressure, and low cost. However, pneumatic tire has some disadvantages as well: low wear drag, large rolling drag, air leak [1].

In order to make up for the shortcomings of the pneumatic tire, non-pneumatic has been widely researched in recent years [2]. Wu [3] designed a new type of non-pneumatic tire with gradient anti-tetrachiral structure and researched that the new tire had good load-carrying capacity. Evangelia [4] designed a parametric finite element NPT model with the honeycomb structure to study its pressure and maximum vertical displacement. Rugsaj [5] developed a finite element NPT model with different spoke shapes to study the geometric effects on the NPT for the maximum stiffness and minimum local stress. Hryciow [6] researched that an increase in the curvature of the spokes reduced radial stiffness and increased the length of the contact path by the numerical tests. Jin [7] investigated the static and dynamic behaviors of NPT with different honeycomb spokes and found that the maximum stresses in spokes and tread of a NPT are much lower than that of traditional pneumatic tires, but its load carrying capacity is higher than the latter. Suvanjumrat [8] proved that the optimum design of NPT to have required load carrying capacity and vertical stiffness can be easily achieved by mean of static Finite Element Method. Aboul-Yazid [9] researched that the shape of the spokes has a great effect on the tire's behavior without a composite ring.

In addition, automobile aerodynamic characteristics have a direct impact on the dynamics, fuel economy and handling stability of the automobile. As an important part of the automobile body, the wheel has an important influence on aerodynamic characteristics of the whole vehicle. Due to the effect of the wheels, the flow field under the vehicle body is further complicated [10,11], and the result also directly affects the aerodynamic characteristics of the vehicle.

The effects of the external flow field of the wheel have been studied at home and abroad, and the cylindrical wheel is usually used as the research object. Axon and Garry [12,13] used CFD fluid simulation software to carry out numerical simulation and wind tunnel experimental analysis of the simplified independent tire, explored the aerodynamic characteristics of the tire in contact with the ground, compared the numerical simulation results with wind tunnel test data, and verified the accuracy of CFD numerical simulation calculation. Fu and Hu [14] simulated the flow field around a single wheel with different spokes by CFD technique and proved that the changes in geometric parameters of wheels affected not only the local flow around wheels but also the characteristics of flow field of whole vehicle. Regert and Lajos [15] analyzed the flow field of cylindrical wheel and wheel housing, carried out simulation and experimental research, and compared. The external

* e-mail: lihong@yzu.edu.cn

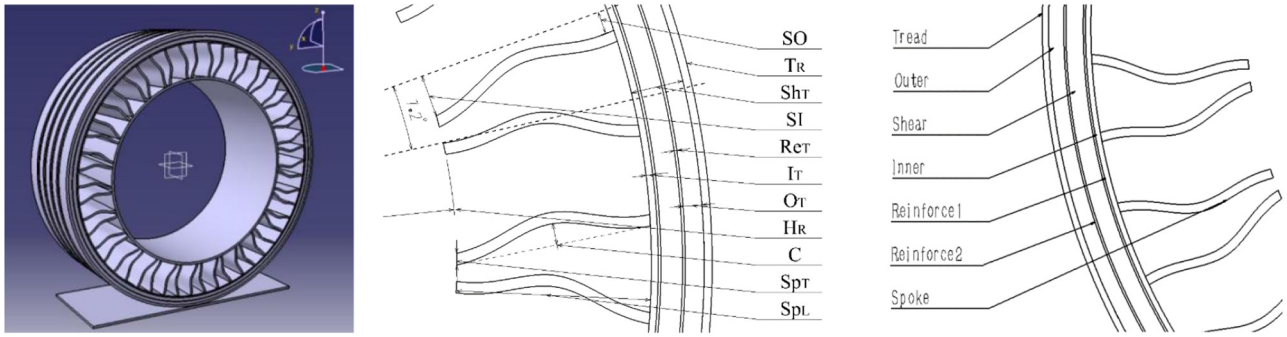

Fig. 1. The original 3D NPT model.

Table 1. Dimension parameters of the original NPT model.

Parameters	Dimension
Tread outside diameter (TR)	600 mm
Rim outer diameter (HR)	410 mm
Tire width (B)	195 mm
Shear zone thickness (ShT)	20 mm
Stiffener thickness (ReT)	1 mm
Thickness of outer shear cover (OT)	7 mm
Thickness of internal shear cover (IT)	3 mm
Number of spokes (Q)	25 pairs
Spoke width (SpB)	193 mm
Spoke thickness (SpT)	4.2 mm
Radial length of spoke (SpL)	72 mm
Spoke curvature (C)	8 mm
Deviation rate of inner side of spoke (SI)	0.6 mm
Deviation rate of outer side of spoke (SO)	0.15 mm

flow field of the wheels under stationary and rotating conditions was numerically simulated by using Fluent software in Tan and Zhang's [16] research, and comparative analysis was carried out. The simulation results showed that the rotating wheel affected the aerodynamic drag and lift of the whole vehicle. Researches show that aerodynamic resistance caused by wheels can account for 30% of the vehicle resistance [17]. Therefore, understanding the characteristics of the flow field near the wheel and the impact on the external flow field of the vehicle plays an important role in further improving aerodynamic characteristics of the whole vehicle. However, previous research typically only investigated the external flow field of the wheel with traditional pneumatic tire. The effect of aerodynamic characteristics of NPT has not been studied extensively.

This paper aims to develop a framework to research the influence of NPT structures on aerodynamic characteristics by numerical simulation and investigate the effects of NPT on the vehicle resistance by wind tunnel test, which can provide a theoretical basis for the design of non-pneumatic tire.

2 Model establishment and numerical calculation theory

2.1 Establishment of tire finite element model

Based on the study of the structural parameters of non-pneumatic tire [2,5,18], the original three-dimensional tire model was established by CATIA software (see Fig. 1). The dimension parameters of the tire are listed in Table 1.

2.2 Static mechanical properties of the original mode

Abaqus software was used for the model mesh and mechanical simulation. A vertical downward concentrated force of 3665 N was applied to the center of the rim, implicit calculation was used, and the change of the tire radial displacement was monitored. The model mesh and simulation result are shown in Figure 2, and the change of the tire radial compression is shown in Figure 3.

Table 2 shows the comparison between the analysis results of this model and the model researched by Akshay Narasimhan [19]. From the comparison of the data in the table, it can be seen that the open non-pneumatic tire model has credibility and can support the subsequent research of the paper.

2.3 Establishment of out flow field model

The NPT model was meshed by ANSYS software. The tire surface was divided into triangular hybrid mesh, and the complex parts were refined by mesh. The flow field area was divided into global tetrahedral unstructured mesh. In order to reduce computation load, half tire model was used for simulation analysis. The parameters of flow field calculation area are listed in Table 3. Flow field calculation domain is shown in Figure 4. Referring to the research of Axon [12,13], a rectangular grounding area of 20° at the contact of tire and ground was used, as shown in Figure 5.

The numerical simulation simulated that the tire rotated around the center axis of the tire at a speed of 80 km/h on the road when the wind speed was 22.22 m/s and the wheel rotary speed was 74.07 rad/s.

The flow field boundary condition parameters were as follows: the wind speed in inlet was 22.22 m/s in the positive Y direction, the turbulent initial boundary condition

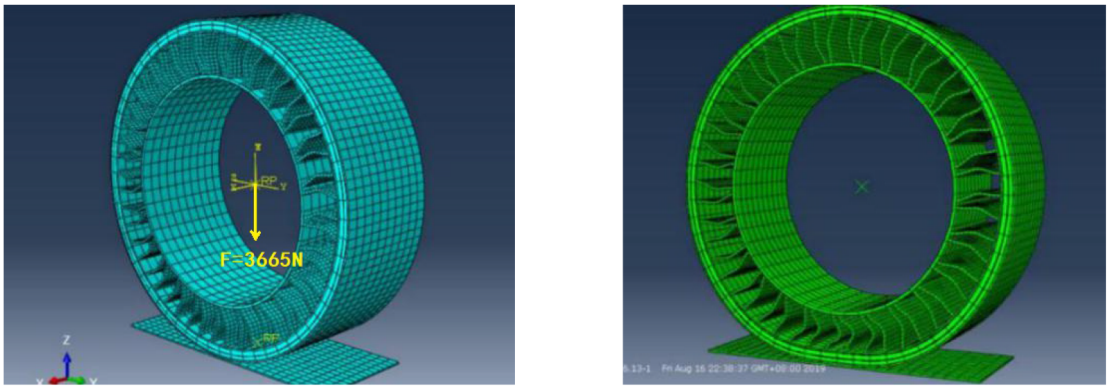

Fig. 2. The original model mesh and simulation diagram under load.

adopted the turbulent kinetic energy k and the turbulent kinetic energy dissipation rate ε, the outlet was pressure-out, the tire was without sliding surface and rotated around the X axis, the ground and wall surface adopted no-sliding surface, the wind speed in outlet was 22.22 m/s in the positive Y direction, and Y-Z face was symmetrical.

2.4 Theory of aerodynamic characteristics

Aerodynamic force refers to three forces along the coordinate axis and three moments around the coordinate axis [20] when the vehicle drives along the positive X axis. Aerodynamic drag F_W (N) in the positive direction of X axis, aerodynamic lift F_L (N) in the positive direction of Z axis, and horizontal lateral force F_S (N) in the positive direction of Y axis. Aerodynamic coefficients can be described through formulas such as the following.

$$\text{Drag coefficient}: C_D = \frac{2F_W}{\rho v_\infty^2 A} \tag{1}$$

$$\text{Lift coefficient}: C_L = \frac{2F_L}{\rho v_\infty^2 A} \tag{2}$$

$$\text{Side forcecoefficient}: C_S = \frac{2F_S}{\rho v_\infty^2 A} \tag{3}$$

where $\rho v_\infty^2/2$ is the dynamic pressure of the air flow; A is the positive projection area of the vehicle; C_D is the drag coefficient; C_L is the lift coefficient; C_S is the side force coefficient.

3 Aerodynamic performances of NPT with different structures

3.1 Numerical simulation of original model

3.1.1 Aerodynamic characteristics of original model

The aerodynamic characteristics of the NPT model were simulated by FLUENT software. The realizable K-ε turbulence model was used for simulation calculation and monitoring the drag and lift of the tire. Scalable wall functions were used for convergence. The moving wall method was used to simulate the forward rolling of tire. The simple pressure-velocity coupling method was selected as the solution method, and the standard second-order upwind discrete method was used for high precision calculation. The convergence factors of K and ε were set to be $\mathbf{10^{-4}}$, and the constant iteration steps were set to be 1500.

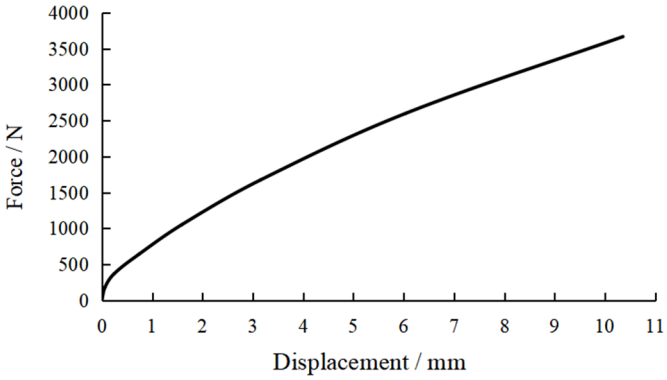

Fig. 3. Change of radial compression of open non-pneumatic tire.

Table 4 presents the simulation results of the drag coefficient and lift coefficient of the original non-pneumatic tire model under static and rotating conditions, and the relative deviation with the research results of other papers. The deviation of simulation results in this paper is close to that of the model researched by Heo [21] under the rotating condition of 14 m/s driving speed, while the simulation results are quite different from those of the pneumatic tire model studied by Axon et al. [12], which means that the spoke structure of the NPT model results in the increase of aerodynamic force. So a set of spokeless tire model was added in this paper for comparison. It can be seen from Table 4 that under rotating conditions, the difference in drag coefficient between the spokeless tire model and the pneumatic tire model (Axon [12]) is only 1.32%, and the difference in lift coefficient is 0.21%, so the model of NPT researched in this paper is feasible. At a rotating speed of 22.22 m/s, the drag coefficient of NPT is 30.16% higher

Table 2. Comparison of static characteristics of non-pneumatic tire models.

Comparison	Load (N)	Radial displacement (mm)	Vertical stiffness (KN/m)
Akshay Narasimhan [19]	3665	10.29	356.17
NPT in this paper	3665	10.36	353.76
Deviation	0%	0.68%	–0.68%

Table 3. Dimension parameters of flow field calculation area.

Size design	Measurement value / mm
Length	14.5
Width	2
Height	4
Wheel center to inlet face	4

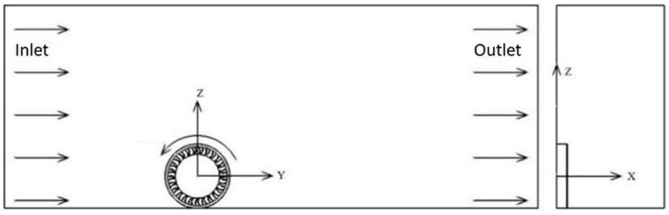

Fig. 4. Flow field calculation domain.

than that of spokeless tire, and the lift coefficient is 7.75% higher because the open spokes cause the aerodynamic coefficient to increase, especially drag coefficient.

3.2 Effects of original model structure on aerodynamic characteristics

The main structural parameters of the NPT model include tire width and spoke parameters. Spoke parameters include the length, thickness, curvature, and spoke offset. The structural parameters of tire were researched and the effect of tire structure on aerodynamic characteristics was analyzed in the following sections.

3.2.1 Effects of tire width

The effect of tire width on aerodynamic characteristics was analyzed in this section. The tire width was reduced respectively by 20 mm, 40 mm, and 60 mm while the tread width was reduced separately by 10 mm and 20 mm. Five models above were used for simulation.

Table 5 presents that when the tire width decreases, the drag coefficient and lift coefficient of the tire gradually decrease; when the tread width decreases, the drag coefficient and lift coefficient of the tire also decrease. The decrease of the tread width has a great effect on the drag coefficient and lift coefficient.

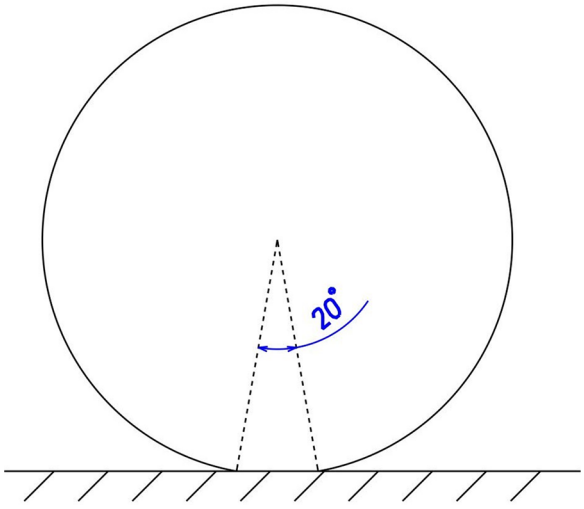

Fig. 5. Grounding area.

3.2.2 Effects of spoke length

When the length of the spokes changes, the volume of the spoke cavity changes, thus the interaction between spokes and air mass in the cavity changes as well. According to the tire model, the spoke length was set to 52 mm, 62 mm, 72 mm, 82 mm, and 92 mm respectively. The simulation results of the aerodynamic characteristics of the five spoke length models are shown in Figure 6.

Figure 6 shows that the decrease of the spoke length results in the decrease of the tire drag coefficient and lift coefficient.

3.2.3 Effects of spoke thickness

The change in the thickness of spoke was 2 mm, thus four schemes was used. Table 6 shows the effect of spoke thickness on aerodynamic characteristics.

Table 6 presents that with the increase of spoke thickness, the drag coefficient has a significant decrease trend, and the lift coefficient has a mild decrease trend.

3.2.4 Effects of curvature and deflection of spokes

The spoke curvature of the original tire model was 8, and the inner and outer offsets of the spoke were 0.6 and 0.15 respectively. Five comparative test schemes for the spoke curvature were as follows: the curvature was 4, 6, 8, 10, and 12 in turn. Four schemes for the spoke offset rate were as follows: the inner /outer offset rate was 0/0, 0.2/0.05, 0.4/0.1, and 0.6/0.15 in turn. The original tire model belonged to curvature scheme 3 and offset scheme 4.

Table 4. Comparison of simulation results of aerodynamic characteristics of the model.

Tire model	State	Speed /m·s^{-1}	Drag coefficient (CD)	Deviation Δ%	Lift coefficient (CL)	Deviation Δ%
NPT model in this paper	Static	14.00	0.895	–	0.595	–
		22.22	0.901		0.610	
	Rotating	14.00	0.783	–	0.501	–
		22.22	0.794		0.514	
NPT model (Heo [21])	Static	14.00	0.868	3.11	0.618	–3.72
	Rotating	14.00	0.774	1.16	0.513	–2.34
Pneumatic tire model (Axon [12])	Static	18.60	0.707	26.59	0.630	–5.56
	Rotating	18.60	0.602	30.07	0.476	5.25
Spokeless tire model	Rotating	22.22	0.610	30.16	0.477	7.75

Table 5. Aerodynamic characteristic coefficients of different spoke lengths.

Width / mm	Drag coefficient (CD)	Deviation Δ%	Lift coefficient (CL)	Deviation Δ%
Tire width 195	0.794	–	0.514	–
Tire width 175	0.768	–3.27	0.468	–8.95
Tire width 155	0.740	–6.80	0.414	–19.46
Tire width 135	0.706	–11.08	0.351	–31.71
Tread width 185	0.751	–5.42	0.480	–6.61
Tread width 175	0.702	–11.59	0.427	–16.92

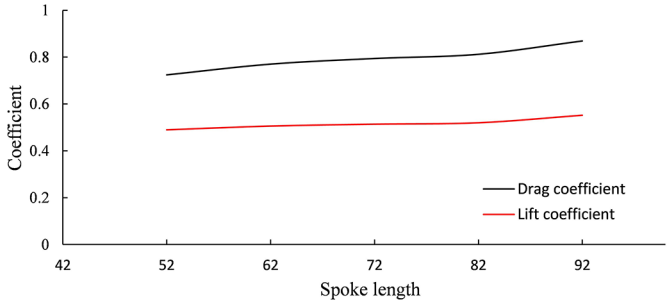

Fig. 6. Aerodynamic coefficients of different spoke lengths.

The results of aerodynamic simulation of the spoke curvature and spoke offset rate are shown in Figure 7.

Figure 7 shows that the change of spoke curvature and spoke deflection rate has few effects on aerodynamic characteristics.

3.2.5 Effects of spoke arrangement

From the research point of view, the spoke length and thickness have obvious influence on the aerodynamic characteristics of open non-pneumatic tires.

Figure 8 shows a pair of spokes with Spoke 1 and Spoke 2. Divide the spokes 1 and 2 of each pair of spokes into 3 sections, 5 sections and 7 sections horizontally. The four section arrangement schemes are shown in Figure 8a. The spoke segments will affect the air flow in the spoke cavity and the force of each spoke. When the tire rotates, it reduces the force of the spokes on the air in the cavity.

Table 7 shows the segment length and radial displacement of the four segmentation schemes. The segmentation of the spokes has a greater impact on the static characteristics of the tire, and the radial displacement of the tire is approximately doubled.

4 Aerodynamic performances of NPT under driving condition

4.1 Effects of traffic speed on aerodynamic characteristics

According to the formulas of the drag coefficient (1) and lift coefficient (2), the square of traffic speed is inversely proportional to the aerodynamic coefficient. Assuming that the tire is under a certain force, the larger the speed is, the smaller the aerodynamic coefficient is. However, in fact, the aerodynamic force is affected by traffic speed as well: the increase of the speed results in the increase of the force of the wind on the tire. So it is difficult to determine the change relationship between the coefficients and variables from formulas. It is necessary to simulate the tire model and further study the effect of different speed on tire aerodynamic characteristics.

The tire model was simulated when traffic speed was 40 km/h, 50 km/h, 60 km/h, 70 km/h, and 80 km/h. The results of simulation were as follows.

Table 6. Effects of spoke thickness on aerodynamic characteristics.

Spoke thickness/mm	Drag Coefficient (CD)	Deviation Δ%	Lift Coefficient (CL)	Deviation Δ%
2.2	0.798	0.50	0.518	0.78
4.2	0.794	–	0.514	–
6.2	0.778	–2.02	0.509	–0.97
8.2	0.772	–2.77	0.509	–0.97

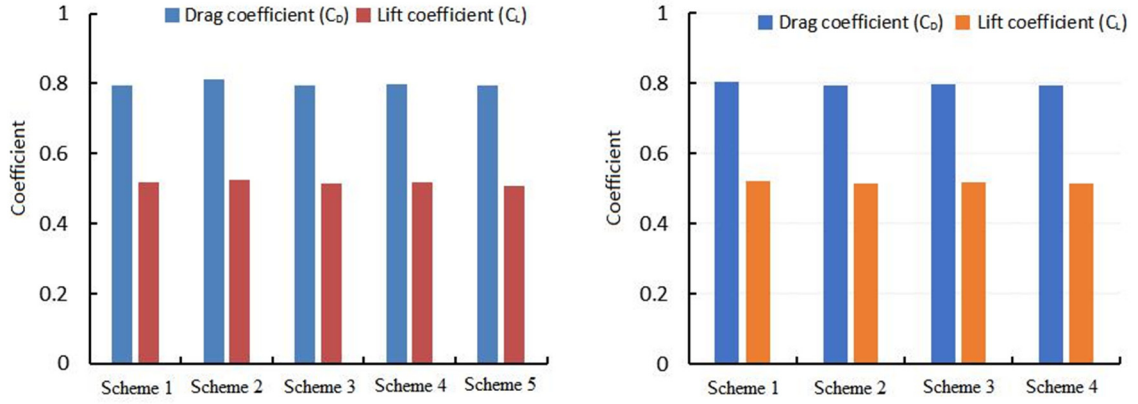

Fig. 7. Effects of the spoke curvature and offset on aerodynamic characteristics. (a) Spoke curvature. (b) Spoke offset.

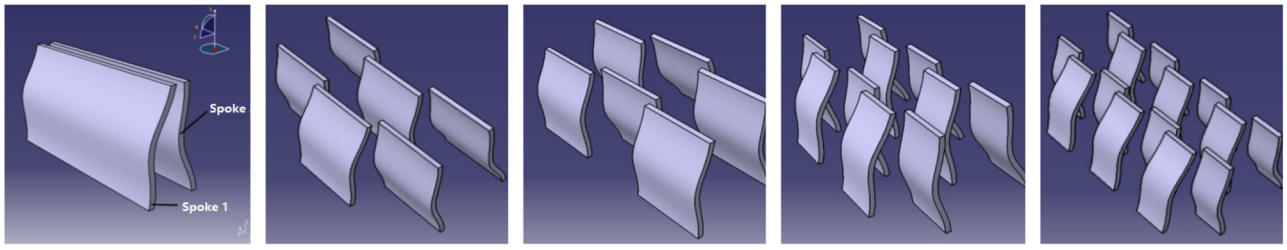

Fig. 8. A pair of spokes (a) and 4 schemes of spoke arrangement (b, c, d, e). (a) A pair of spokes. (b) Scheme 1. (c) Scheme 2. (d) Scheme 3. (e) Scheme 4.

Table 7. Size of spoke arrangement schemes and radial displacement.

Scheme	Spoke			Radial displacement/mm
	Segment	Spoke 1	Spoke 2	
Origin	1	195	195	10.36
Scheme 1	3	65	65+65	20.44
Scheme 2	3	65+65	65	20.41
Scheme 3	5	39+39	39+39+39	20.81
Scheme 4	7	29+29+29	27+27+27+27	20.89

Table 8 shows that, as the aerodynamic coefficients increase slightly with a positive correlation trend. Combined with the analysis of the aerodynamic formulas, as traffic speed increases, the aerodynamic force on the tire increases as well.

4.2 Effects of tires on aerodynamic characteristics of the whole vehicle

The simulation and analysis of aerodynamic characteristics of independent tire models at different traffic speed have been carried out. With the addition of the body model,

Table 8. Effects of traffic speed on pneumatic characteristics of tire.

Speed (km/h)	Drag coefficient (CD)	Deviation Δ%	Lift coefficient (CL)	Deviation Δ%
80	0.794	–	0.514	–
70	0.791	–0.38	0.511	–0.58
60	0.789	–0.63	0.508	–1.17
50	0.781	–1.64	0.499	–2.92
40	0.779	–1.89	0.494	–3.89

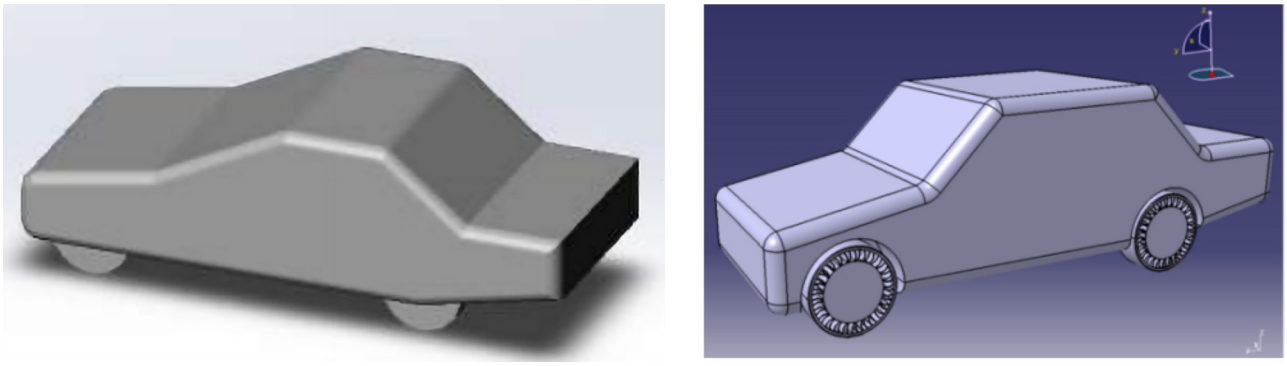

(a) (b)

Fig. 9. MIRA model [20] and the improved vehicle model. (a) MIRA model. (b) The improved vehicle model.

the flow field of the vehicle model is different from that of the independent tire model, and the body and the tire interact with each other.

MIRA model [22] was used to improve the size of the vehicle body as shown in Figure 9a. The improved vehicle model with 4 NPT wheels is shown in Figure 9b.

Two kinds of vehicle simulation models were established: one was with solid tire, the other was with NPT. Under the condition that tire rotates, the aerodynamic force and aerodynamic coefficients of the two vehicle models were calculated, as well as the relevant aerodynamic coefficients of the tire. The turbulence profile of the two models on the surface is shown in Figure 10.

The turbulence intensity at the front wheel is larger than that at the rear wheel, as shown in Figure 10. The rotating tire greatly affects the flow field of the whole vehicle. The turbulence intensity at the wheel with NPT is larger than that at the wheel with solid tire, which shows that the open spokes intensify the turbulence movement at the wheel.

Table 9 shows that under the rotating condition, due to the use of NPT, the wind drag coefficient of the whole vehicle model increases by 0.03 and the drag increases by 17.52 N; however, the lift coefficient decreases by 0.014. For the tire, the drag coefficient of NPT increases by 0.01 and the drag increases by 5.72 N, while the lift coefficient decreases by 0.012. In general, the use of NPT increases the wind drag of the whole vehicle model by about 8% while decreased the lift of the whole vehicle model by over 20%. Therefore, NPT wheels can be used for cars to make the grip performance much better and make driving safer.

Table 10 shows the simulation results of aerodynamic characteristics of the whole vehicle model and each part: the tire drag coefficient accounts for 21.21% of that of the whole vehicle model, and the lift coefficient accounts for 26.57%. 63.1% of the drag and 65.79% of the lift are provided by front wheels, which have more drag and lift than the rear wheels. The simulation results basically coincide with the phenomena reflected in Figures 9 and 10.

5 Wind tunnel test

5.1 Structural optimization of the original tire model

Since the curvature of the spokes has little effect on the aerodynamic force, the parameters were selected only for tire width, spoke length, and spoke thickness.

Nine models in Table 11 were simulated under a pressure of 3665 N by Abaqus software. The radial displacement of the tire under load is shown in Figure 11. In order to ensure that the load-bearing capacity of the tire varies within a certain range, the variation range of the tire radial displacement should not exceed 5% (between 9.842 mm and 10.878 mm).

From Figure 11, the models that meet the tire static characteristics are D, G, H, and I, and the radial displacements are 10.410 mm, 10.212 mm, 10.659 mm, and 10.380 mm.

Then aerodynamic simulation was conducted on the selected model and the simulation result is shown in Figure 12. The drag coefficients and lift coefficients of model G, H, I are smaller than the original tire model. Among them, the drag coefficient of model H is the smallest

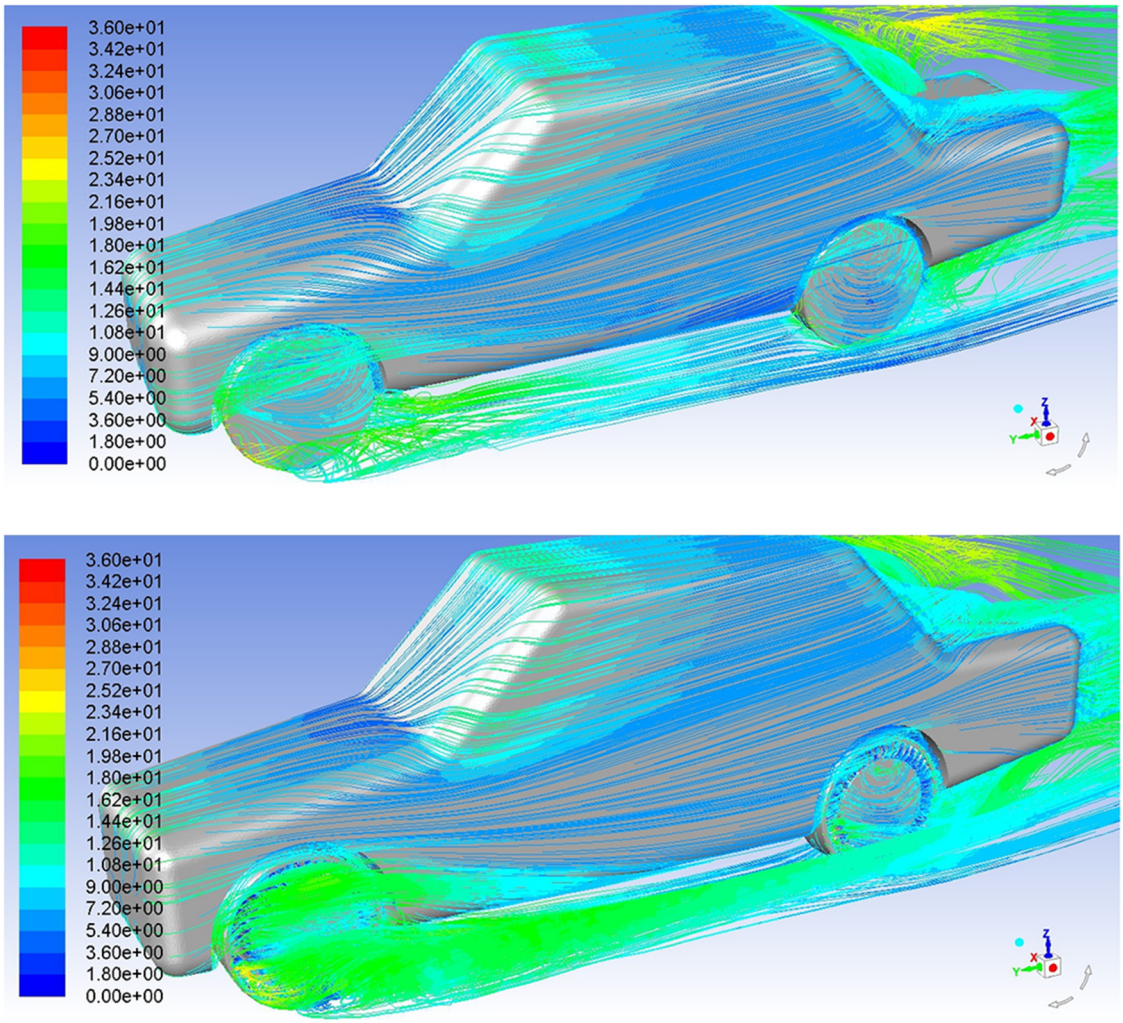

Fig. 10. Turbulence profile of the vehicle with solid tire and NPT.

with a value of 0.757 and the lift coefficient is 0.447. The drag coefficient of D is larger than the original tire model, so it is eliminated.

Finally, the aerodynamic noise simulation on G, H, I was conducted, and the results are shown in Table 12.

Model H meets all the optimization requirements from Figure 13, the drag coefficient and sound pressure level is the smallest, and the lift coefficient is also appropriate. 3D model of optimized model is shown in Figure 14.

Table 13 shows that under the driving condition of 22.22 m/s, the radial displacement of model H has increased by 2.89% compared with the original model, which is within the preset range of 3%. In addition, Model H has a more obvious impact on aerodynamic characteristics of NPT, the aerodynamic drag coefficient is reduced by 4.66%, and the tire lift coefficient is reduced by 13.04%. Under the driving condition of 14 m/s, the aerodynamic drag coefficient of Model H is 3.36% lower than that of Heo model, the lift coefficient is reduced by 15.01%. In general, the optimization of the structural parameters of the model H can achieve the drag reduction effect of non-pneumatic tire.

5.2 Experimental equipment and installation steps

The wind tunnel laboratory in Yangzhou University was funded by the central budget and was officially put into use in 2018. The wind tunnel is a direct current inspiratory wind tunnel, as shown in Figure 15. The wind speed range is 0−40 m/s. The test section of the wind tunnel is 1.0-meter long, 0.4-meter wide, and 0.4-meter high. The effective cross-sectional area of the test section of the wind tunnel is 0.16 m^2.

Because the tire size is large, and the wind tunnel blockage ratio should be less than 15%, the tire model was reduced by a ratio of 1:4 and made by the light curing 3D printer, as shown in Figure 16. The three-dimensional stiffness of 3D printed non-pneumatic tires is basically 50% of that obtained by Wang's simulation [23]. Therefore, the performance of these materials were moderately reduced during the structural design for performance simulation so as to guarantee the prediction of the performance of 3D printed non-pneumatic tires.

Six-component wind tunnel balance was used to monitor the aerodynamic forces in six directions of the

Table 9. Numerical simulation results of aerodynamic characteristics of the vehicle.

Tire type	Total drag coefficient	Total drag/N	Total lift coefficient	Total lift/N	Tire drag coefficient	Tire drag/N	Tire lift coefficient	Tire lift / N
Solid tire	0.366	206.84	0.157	88.64	0.073	41.50	0.049	27.86
NPT	0.396	224.36	0.143	81.06	0.083	47.22	0.037	21.24

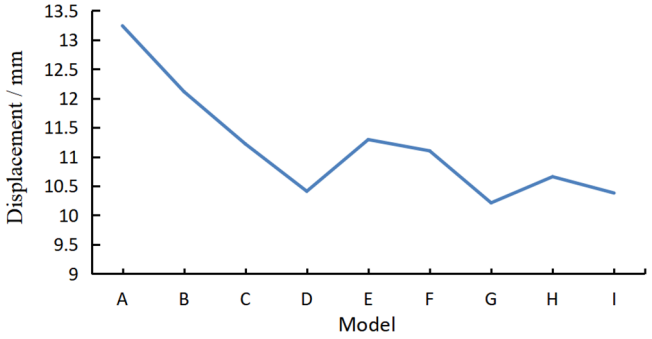

Fig. 11. Structural parameters of the optimized model.

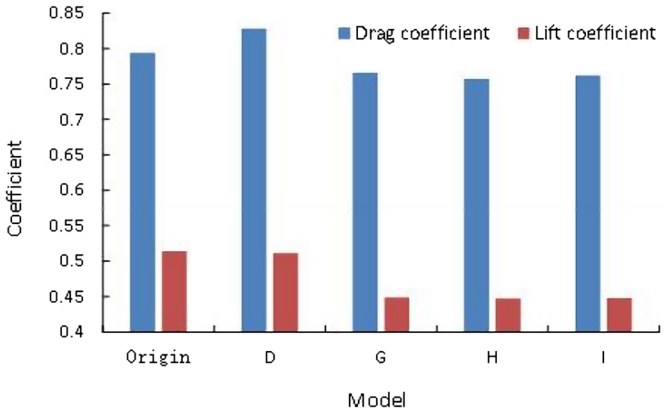

Fig. 12. Aerodynamic characteristics of models.

Table 10. Numerical simulation results of aerodynamic characteristics of parts.

Parts	Drag coefficient	Drag /N	Lift coefficient	Lift /N
Whole vehicle	0.396	224.36	0.143	81.06
body	0.312	177.13	0.105	59.83
front wheel	0.053	29.57	0.025	14.05
rear wheel	0.031	17.66	0.013	7.18

Table 11. Structural parameters of the optimized model.

Model	Tire width/mm	Spoke length/mm	Spoke thickness/mm	Curvature
A	185	67	5	8
B	185	65	5.4	8
C	185	65	5.2	8
D	185	62	5.2	8
E	175	62	5.2	8
F	170	56	5.2	8
G	165	56	5.3	8
H	165	56	5.2	8
I	165	55	5.2	8

tire. During the experiment, the data acquisition device collected the instantaneous force and moment of the tire through the sensor in the six component wind tunnel balance, and transmitted them to the ATI DAQ F/T software on the computer.

Six-component wind tunnel balance was fixed on the floor of the wind tunnel test section, then the transmission line, tire base and NPT were installed in turn. The placement of the model in the wind tunnel is shown in Figure 17.

Experiment 1: The experiment focused on the research of aerodynamic characteristics of tire under the static condition. Wind speed was set to be 11 m/s, 14 m/s, 16 m/s, 19 m/s, and 22 m/s. The instantaneous aerodynamic drag and lift of tire were measured under different wind speed. After the flow field was stable, 500 groups of experimental data were collected.

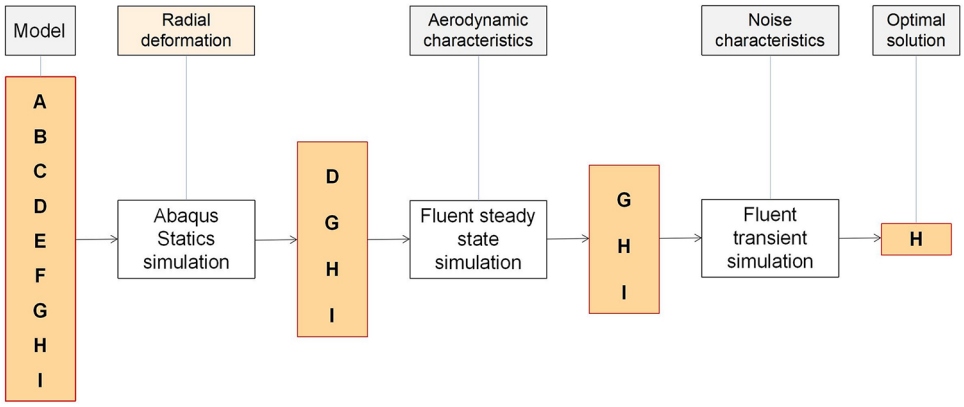

Fig. 13. Tire optimization plan.

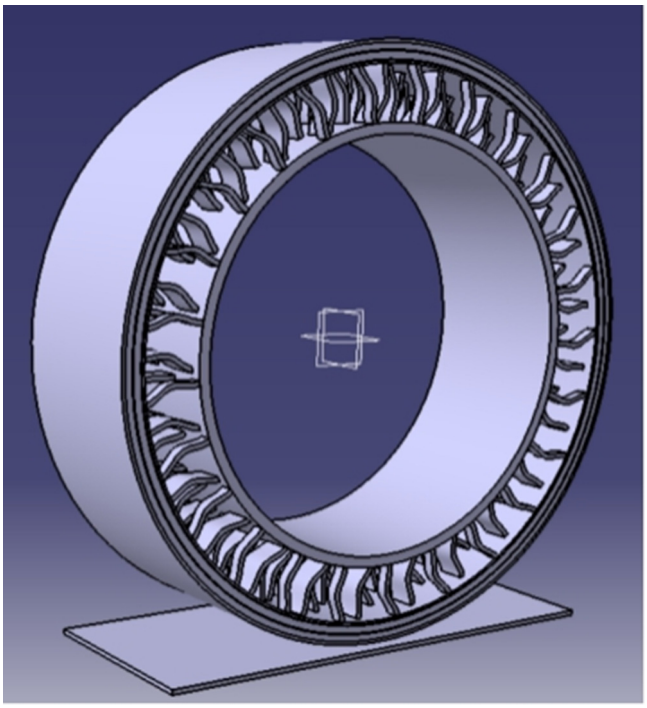

Fig. 14. 3D model of optimized model H.

Fig. 15. Direct current inspiratory wind tunnel.

Fig. 16. 3D printed tire model.

Experiment 2: Open spokes can definitely increase the influence in the wind measurement state. The experiment was to explore the influence of the wind direction angle on the aerodynamic force of NPT at a wind speed of 16m/s. The wind direction angle ranged from 0° to 32°, and transient data was collected every 8°.

5.3 Experiment and verification

The main purpose of the experiment was to monitor the drag and lift of the tire. The mean value of the aerodynamic force would be obtained by sample data. Because the experimental model was installed on the fixed base (as shown in Fig. 18), the part of the force on the base should be corrected and removed according to the area proportion.

Table 12. Sound pressure level of models.

Model	Sound pressure level / dB
G	66.04
H	64.51
I	65.69

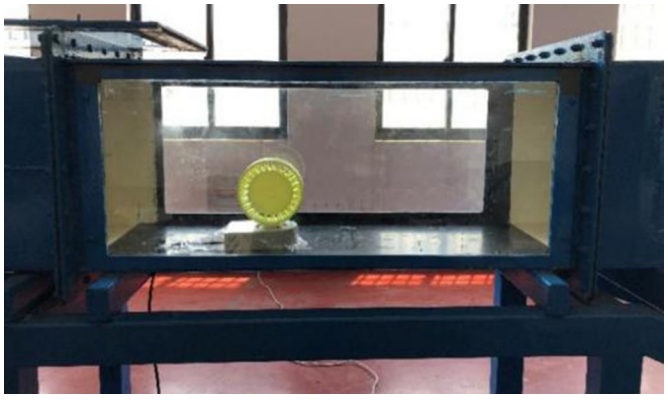

Fig. 17. Tire placement in the wind tunnel.

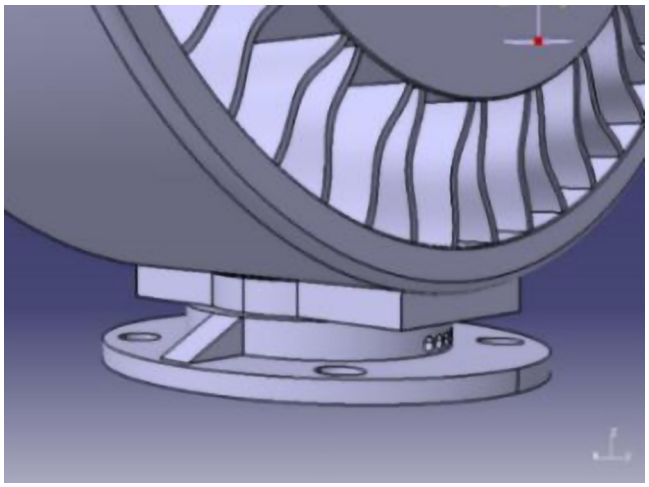

Fig. 18. Fixed base.

Table 13. Comparison of aerodynamic characteristics and radial displacement of the models.

Model	Drag coefficient Cd	Deviation Δ%	Lift coefficient Cl	Deviation Δ%	Radial displacement/mm	Deviation Δ%
Original Model (22.22 m/s)	0.794	–	0.514	–	10.360	–
Model H (22.22 m/s)	0.757	–4.66	0.447	13.04	10.659	2.89
Heo Model (14 m/s)	0.774	–	0.513	–	–	–
Original Model (14 m/s)	0.781	0.9	0.499	–2.73	10.360	–
Model H (14 m/s)	0.748	–3.36	0.436	–15.01	10.659	–

The comparison between the experimental and simulated aerodynamic characteristics of the original model is shown in Table 14 and Figure 19.

Figure 19a and b presents that, as wind speed increases, the tire drag and lift increases as well. And Figure 19c and d presents that, as wind speed increases, aerodynamic coefficient increases slightly, and the change trend of drag coefficient is consistent to that of lift coefficient.

As shown in the figures above, the results of wind tunnel test are larger than the simulation results. The mean difference value ($\overline{C}$) and relative deviation (ΔC) between the tested and simulation results of drag coefficient are calculated by formulas (4) and (5). The mean difference value ($\overline{C}$) and relative deviation (ΔL) between the tested and simulation results of lift coefficient are calculated by formulas (6) and (7).

$$\overline{C} = \frac{1}{n}\sum_{n=1}^{5}(Cs_n - Cf_n), (n = 1, 2, 3, 4, 5) \tag{4}$$

$$\Delta C = \frac{Cs - Cf}{Cf} \times 100\% \tag{5}$$

$$\overline{L} = \frac{1}{n}\sum_{n=1}^{5}(Ls_n - Lf_n), (n = 1, 2, 3, 4, 5) \tag{6}$$

$$\Delta L = \frac{Ls - Lf}{Lf} \times 100\% \tag{7}$$

where n is the number of experimental comparison groups; Cs is the experimental drag coefficient; Cf is the simulated drag coefficient; Ls is the experimental lift coefficient; Lf is the simulated lift coefficient.

According to the experimental data, the mean difference value of drag coefficient is 0.0312, and the mean difference value of lift coefficient is 0.0284. In five sets of control experiments, when wind speed is 11 m/s, the relative deviation of drag coefficient is the largest, which is

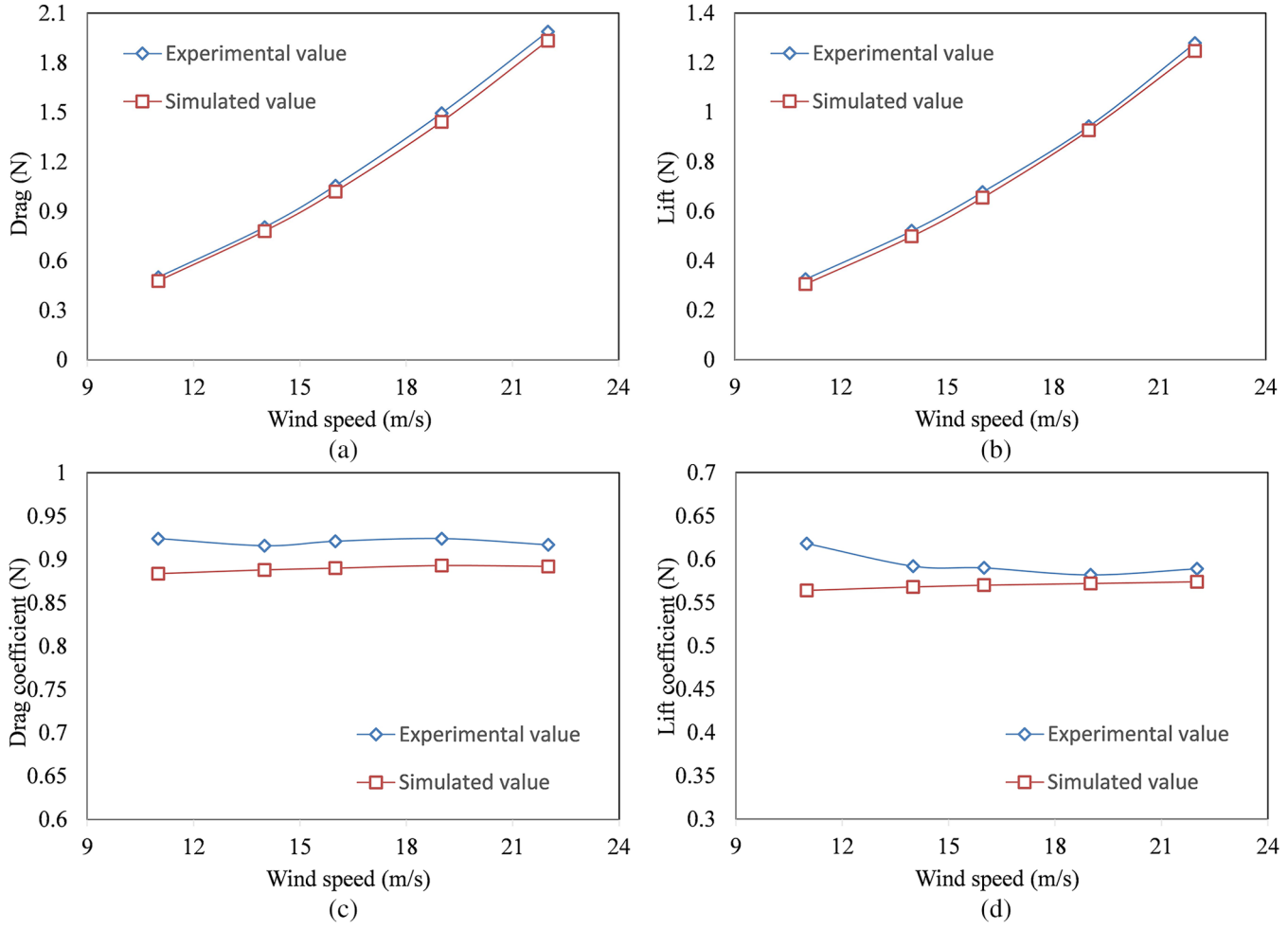

Fig. 19. Experimental and simulated aerodynamic characteristics. (a) Drag. (b) Lift. (c) Drag coefficient. (d) Lift coefficient.

Table 14. Experimental and simulated aerodynamic characteristics of model H.

Wind speed (m/s)	Experiment value				Simulation value			
	Drag/N	Drag coefficient	Lift/N	Lift coefficient	Drag/N	Drag coefficient	Lift/N	Lift coefficient
11	0.404	0.881	0.220	0.481	0.372	0.813	0.216	0.472
14	0.644	0.867	0.379	0.510	0.626	0.843	0.353	0.475
16	0.860	0.886	0.503	0.518	0.819	0.844	0.462	0.477
19	1.160	0.848	0.693	0.506	1.156	0.845	0.654	0.479
22	1.586	0.864	0.935	0.510	1.551	0.845	0.881	0.480

up to 8.36%. The minimum relative deviation of wind drag coefficient is 0.36% when wind speed is 19 m/s. Also, when wind speed is 16 m/s, the relative deviation of lift coefficient reaches the maximum value 8.60%. The minimum relative deviation of lift coefficient is 1.91% when wind speed is 11 m/s.

The experimental deviation of 11 m/s wind speed is the largest, which may be because low wind speed makes the force on the tire small, and there are differences between the printed experimental model and the simulation model. Also, there are differences between the boundary conditions in the experiment and the simulation, for example, the wind speed of the fan is not stable, resulting in the experimental data become larger. Overall, this wind tunnel experiment can verify the reliability of tire numerical simulation.

Under the condition of 16 m/s wind speed, the instantaneous simulation of the original tire model was carried out. Firstly, the tire model was iterated in 1000 steps, and after the flow field reached a stable state, the data of the drag coefficient was collected out in 500 steps. Then, the data of 16 m/s wind speed was collected, and the instantaneous aerodynamic coefficient of tire could be calculated by the formulas (1) and (2).

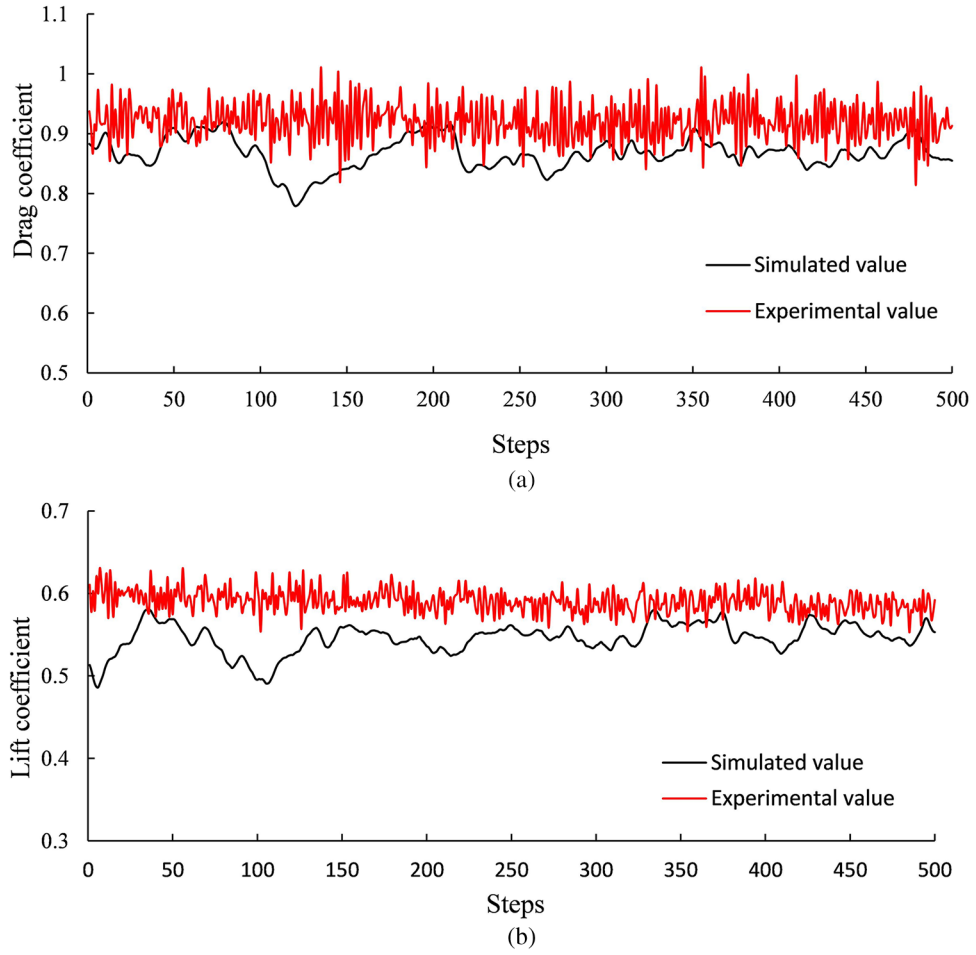

Fig. 20. Instantaneous drag and lift coefficient. (a) Instantaneous drag coefficient. (b) Instantaneous lift coefficient.

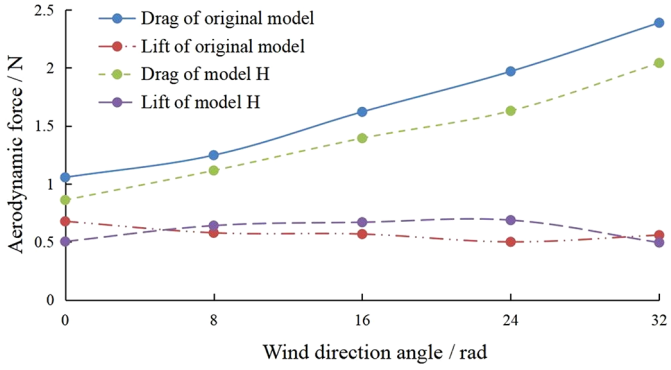

Fig. 21. Aerodynamic forces at different wind angles.

Figure 20a shows that the experimental instantaneous drag coefficient of tire is larger than that of simulation, but the overall trend is similar. The trend of lift coefficient in Figure 20b is similar to that of wind drag coefficient. The fluctuation of lift coefficient is relatively stable in the experiment and simulation. Two figures above can also verify the reliability of the simulation model and the accuracy of the simulation method.

The experiment of the influence of wind direction on tire aerodynamics was to explore the aerodynamic changes of NPT when the vehicle was turning. The wind tunnel experiment was conducted on two tire models with different wind direction angles. The experimental results are shown in Figure 21.

6 Discussion and conclusions

The reduction of tire width and spoke length, and the increase of spoke thickness can effectively decrease the aerodynamic coefficient. Spoke curvature and spoke offset have no influence on the aerodynamic coefficient.

- The increase of traffic speed can slightly increase aerodynamic coefficient. When traffic speed increases from 40 km/h to 80 km/h, the drag coefficient increases by 1.89%.
- Compared with the solid tire, NPT can affect the turbulence state of the whole vehicle model, which increases the drag coefficient of the whole vehicle by 8.20%. The drag of NPT accounts for 21.21% of the whole vehicle, and 65.79% of the tire drag is provided by the front wheel. Therefore, the further design of non-pneumatic tire is required to reduce resistance.

– The wind tunnel test of the original model verifies that the increase of wind speed makes the aerodynamic forces of tire increase.

Conflict of interest

This research received no external funding. The authors declare no conflict of interest.

The authors thank Professor Kun LIANG and Professor Qi Zhang for the assistance with writing skills, and thank Yangzhou University for the use of the wind tunnel facilities.

References

[1] An Gent, Jd Walter, The pneumatic tire (National Highway Safety Administration, Washington, DC, 1985)
[2] P.A. Rangdale, K.R. Chandak, G.M. Bagade, Non pneumatic tyre, Int. J. Eng. Sci. Res. Technol. **2**, 61–68 (2018)
[3] T.Y. Wu, M.X. Li, X.L. Zhu et al., Research on non-pneumatic tire with gradient anti-tetrachiral structures, Mech. Adv. Mater. Struct. (2020)
[4] G.P. Evangelia, P. Chatzistergos, X.X. Wang, The influence of the honeycomb design parameters on the mechanical behavior of non-pneumatic tires, Int. J. Appl. Mech. **12** (2020)
[5] R. Rugsaj, C. Suvanjumrat, Study of geometric effects on non pneumatic tire spoke structures using finite element method. Mechanics based design of structures and machines (2020)
[6] Z. Hryciow, J. Jackowski, M. Zmuda. The influence of non-pneumatic tyre structure on its operational properties, Int. J. Autom. Mech. Eng. **17**, 8168–8178 (2020)
[7] X.C. Jin, C. Hou, X.L. Fan et al., Investigation on the static and dynamic behaviors of non-pneumatic tires with honeycomb spokes, Compos. Struct. **187**, 27–35 (2018)
[8] C. Suvanjumrat, R. Rugsaj, The dynamic finite element model of non-pneumatic tire under comfortable riding evaluation, Int. J. Geom. **19**, 62–68 (2020)
[9] A.M. Aboul-Yazid, M.A. Emam, S. Shaaban et al., Effect of spokes structures of characteristics performance of non-pneumatic tires, Int. J. Autom. Mech. Eng. **11**, 2212–2223 (2015)
[10] H.B. Huang, X.D. Yu, Q.G. Liu et al., Numerical simulation for airflow field around car wheels [J], J. Syst. Simulat. **31**, 641–647 (2019)
[11] B. Peter, S. Simone, B. Alexander, Effects of wheel configuration on the flow field and the drag coefficient of a passenger vehicle, Int. J. Autom. Technol. **20**, 763–777 (2019)
[12] L. Axon, K. Garry, J. Howell, An evaluation of CFD for modelling the flow around stationary and rotating isolated wheels, SAE Trans. **107**, 205–215 (1998)
[13] L. Axon, K. Garry, J. Howell, The influence of ground condition on the flow around a wheel located within a wheelhouse cavity, SAE Technical Paper 01–0806 (1999)
[14] L.M. Fu, X.J. Hun, S.C. Zhang, A research on numerical simulation for the flow field around automotive wheels with different geometric parameters, Autom. Eng. **28**, 451–454 (2006)
[15] T. Regert, T. Lajos, Description of flow field in the wheelhouses of cars, Int. J. Heat Fluid Flow **28** (2007)
[16] Y.W. Tan, Z.H. Zhang, Q.S. Liu, Analysis of automobile external flow field with the influence of rotating vehicle wheel based on fluent, J. Sichuan Univ. Sci. Eng. (Natural Science Edition) **28**, 17–21 (2015)
[17] X.L. Liu, X.X. Yan, S.R. Huang, Numerical research on influence of the underbody flow structure of automotive Aerodynamic performance, J. New Industr. **5**, 35–41 (2015)
[18] Y.J. Deng, Y.Q. Zhao, F. Lin et al., Simulation of steady-state rolling non-pneumatic mechanical elastic wheel using finite element method, Simul. Model. Pract. Theory **85**, 60–79 (2018)
[19] A. Narasimhan, A computational method for analysis of material properties of a non-pneumatic tire and their effects on static load-deflection, vibration, and energy loss from impact rolling over obstacles, Clemson University, 2010
[20] S. Bezgam, Design and analysis of alternating spoke pair concepts for a NPT with reduced vibration at high speed rolling. Clemson University, 2009
[21] H. Heo, J. Ju, D.M. Kim et al., A study on the aerodynamic drag of a NPT [A]. ASME International Design Engineering Technical Conferences and Computers and Information in Engineering Conference **6**, 517–521 (2012)
[22] Y.C. Zhang, J.T. Zhang, K.G. Wu, Aerodynamic characteristics of mira fastback model in experiment and CFD, Int. J. Autom. Technol. **20**, 723–737 (2019)
[23] J. Wang, B. Yang, X. Lin et al., Research of TPU materials for 3D printing aiming at non-pneumatic tires by FDM method, Polymers **12**, 2492 (2020)

Cite this article as: H. Li, Y. Xu, C. Si, Y. Yang, A research on aerodynamic characteristics of non-pneumatic tire, Mechanics & Industry **22**, 27 (2021)